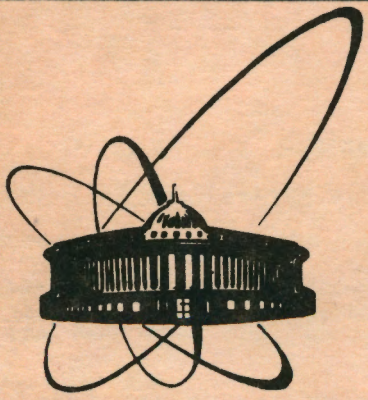

сообщения
объединенного
института
ядерных
исследований
дубна

E13-91-193

V.N.Polushkin, A.G.Likhachev

THE THERMAL NOISE IN HIGH-T_c RF SQUIDs.
I. Experimental Technique

1991

Using high-T_c SQUIDs scientists have already received the series of interesting scientific and technical results [1-3]. However, up to the present time detailed experimental investigations of noise characteristics in such SQUID systems have not been realized yet. It is rather difficult to make unambiguous estimations in this question, as we do not know exactly the interferometer own flux noise. It is clear, the noise model created for niobium SQUIDs can not be transferred automatically to the high-T_c SQUIDs because the main condition of its applicability

$$L_s \ll L_f \qquad (1)$$

is not executed, where L_s is the inductance of the interferometer,

$L_f = \phi_o/(2\pi)^2 k_b T$ is the fluctuation inductance indicating the limit for L_s at exceeding of which interference properties of SQUIDs are damping exponentially ($\sim\exp(L_s/L_f)$) [4]. ϕ_o = 2.07 10^{-15} Wb, k_b is the Boltzman constant, T is the interferometer noise temperature.

In this work we try to estimate, in a preliminary way, the contributions of main noise sources to the SQUID system experimentally. Here, in the first part of the paper (Experimental technique), we intend only to describe methods, function and basic circuits of units which were essential to carry out experiments of such kind. Necessary comments on the experimental results and their comparison with the theoretical model will be given later in the second part of the article (The discussion of experimental results).

The function scheme of the SQUID system

We will consider the function scheme of the SQUID system which is represented in fig.1. In fig.1 L_s is a superconducting quantum interferometer, G_{rf} is the generator of rf-current bias , L_TC_T is the tank circuit reading the information from the interferometer, A is a low-noise rf-amplifier, D,C,R is the amplitude detector.

The total spectral density of magnetic flux noise in the system [5] is

$$S_\phi^\Sigma = S_\phi^i + S_\phi^p + S_\phi^{tc}, \qquad (2)$$

where S_ϕ^i, S_ϕ^p, S_ϕ^{tc} are the equivalent spectral noise densities of the interferometer, amplifier, and tank circuit correspondingly referred to the interferometer input.

Only experimentally S_ϕ^Σ and $S_\phi^p + S_\phi^{tc}$ can be measured. But if the noise temperature of tank circuit T_{tc} is known we can determine S_ϕ^p from the sum $S_\phi^{tc} + S_\phi^p$.

According to [6]:

$$S_\phi^p = 2\pi\alpha^2 k_b T_p L_s \gamma_c / (1-\alpha)^2 \omega_{rf}, \qquad (3)$$

where T_p is the noise temperature of the amplifier, α is the slope parameter for "plato" of rf-voltage-current characteristic (VIC), introduced by Jackel and Buhrman in [6], $\omega_{rf}/2\pi$ is the pumping frequency, γ_c is the parameter reflecting the influence of nonsinusoidality of the current-phase relation in the Josephson junction on the SQUID characteristics.

$$S_\phi^{tc} \simeq 2\pi\alpha^2 k_b L_s T_{tc} \gamma_c / (1-\alpha)^2 \omega_{rf}, \qquad (4)$$

where T_{tc} is the noise temperature of the tank circuit.

Further we will focus our attention on the discussion of methods and technique which were used to determine mentioned above parameters in expressions (2),(3),(4).

The main parameters of the interferometer

The methods developed for the determination of the interferometer parameters, such as, L_s were given in [7]. In this paper we will simply join all these parameters and give them in table 1.

Table 1

The inductance of SQUID, L_s, H	$1.1\ 10^{-10}$
The main parameter, $l = 2\pi L_s I_c/\phi_o$	1
The slope coefficient of "plato", α	0.46
RF-bias frequency, $f_{rf}=\omega_{rf}/2\pi$, MHz	20
Quality factor of L_TC_T, Q	51
Mutual inductance, M, nH	1.77
Inductance L_T, μH	0.64

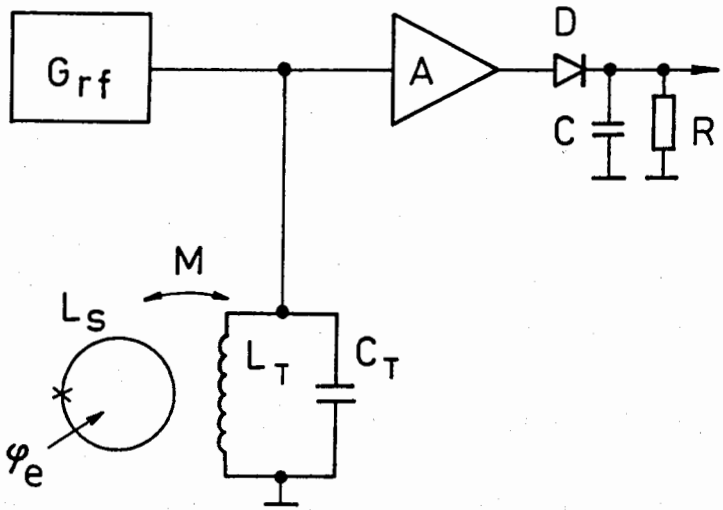

Fig. 1. The function scheme of the SQUID system. L_s is superconducting quantum interferometer, G_{rf} is the generator of rf-current bias, L_TC_T is resonant tank circuit reading the information of interferometer, A is the low-noise FET cascode input preamplifier, DCR is the amplitude detector.

The low-noise rf-amplifier

In our experiments we used cooled rf-preamplifier. It was built as a cooled one not only to decrease its own voltage noise level. We pursued mainly two purposes:

a) to be more precise in the estimation of noise temperature of tank circuit, T_{tc}. In systems with room rf-preamplifiers T_{tc} is unknown because of capacitance C_k of coaxial line connecting the amplifier with L_TC_T and of the input capacitance of the amplifier, C_p. Capacitances C_k and C_p referred to are the parts of C_T but they have the temperature somewhere between 78K and 300K. Besides, the temperature of C_k changes during the evaporation of liquid nitrogen.

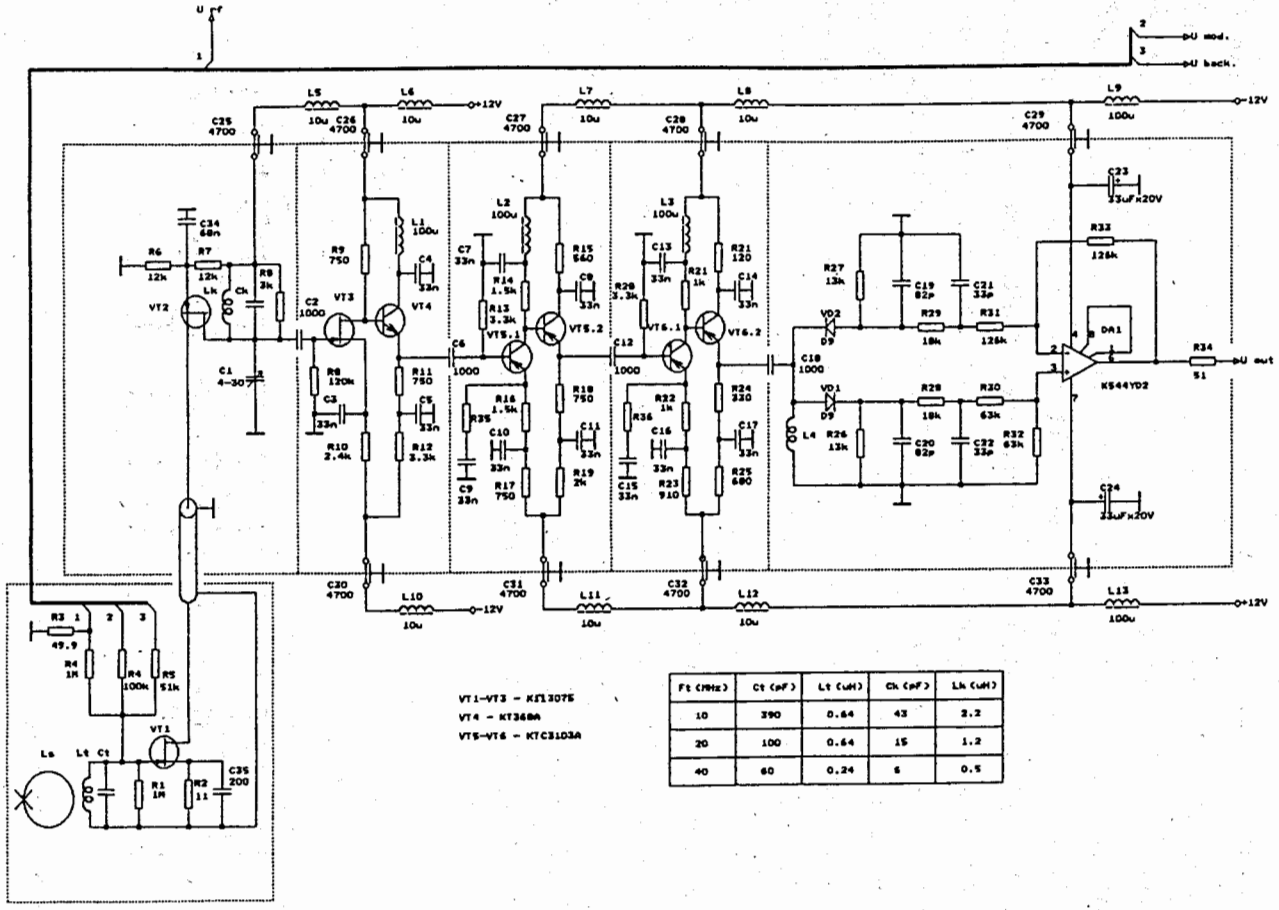

Ft (MHz)	Ct (pF)	Lt (uH)	Ck (pF)	Lk (uH)
10	390	0.64	43	2.2
20	100	0.64	15	1.2
40	60	0.24	5	0.5

Fig.2. Schematic diagram of the low-noise preamplifier.

b) not to consider rf-cable noise which, as noted in [8], can be substantial in the system total noise .

The schematic of the amplifier is represented in fig.2. The interferometer L_s was inductively coupled to the tank circuit, L_TC_T, which, in its turn, was connected to the unipolar transistor VT1 of the amplifier first stage directly (without the rf-coaxial line). All these elements were placed at the liquid nitrogen temperature, ~78K. The first stage represents the cascode connection of the VT1 and VT2 with resonant loading circuit, L_kC_k. The noise characteristics of such kind a cascade were studied by the autors of [8,9] in detail. But in our case there is a peculiarity, as we can see in fig.2: the lower transistor VT1 is placed at T=78K, whereas the upper transistor VT2 works at the room temperature, and they are connected by the coaxial line with the length about 30 cm and, consequently, with considerable capacitance C. It is interesting to examine the influence of this peculiarity on the noise properties. Here we will calculate the noise from the VT1 and VT2 assumed to be predominant.

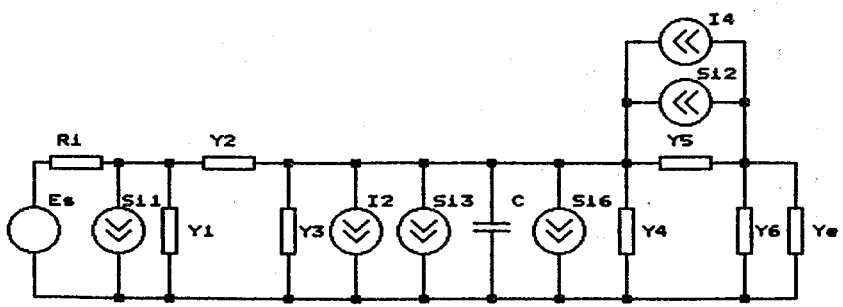

Fig.3. The noise equivalent circuit of the cascode input stage.

The noise equivalent circuit of the cascode input stage is given in fig.3 [10]. E_s is the signal source with an output resistance R_i, S_{i1} and S_{i6} are spectral current noise densities of the VT1- and VT2 gates created by distributed voltage noise of channels through capacitive coupling of channels with gates.

$$S_{i1} = 4k_bT'_ot_gg'_{11}, \qquad S_{i6} = 4k_bT''_ot_gg''_{11}, \qquad (5)$$

where t_g is the relative noise temperature of the unipolar transistor gate (t_g is from 1 to 1.3) [10], T'_o, T''_o are physical temperatures of VT1 and VT2, correspondingly, g'_{11}, g''_{11} are active parts of the input conductances for the VT1 and VT2 respectively.

$$S_{i3} = 4k_bT'_dt_cS_1, \qquad S_{i5} = 4k_bT''_dt_cS_2, \qquad (6)$$

where t_d is the relative noise temperature of the drain (t_d is from 0.5 to 1) [10], S_1, S_2 are the transconductions of the VT1 and VT2, respectively.

$$S_{i4} = S_2S_{v2} / (1+S_2r_s), \qquad (7)$$

where S_{V2} is the spectral density of voltage noise on the source-gate electrodes of VT2, $r_s = 0.2 /S_2$.

Over frequency range from 10 to 40 MHz the parameters of the equivalent scheme are :

$$y_1=j\omega_{rf}C_{gs}, \qquad y_2=j\omega_{rf}C_{gd}, \qquad y_3=1/r_{ds},$$
$$y_4=j\omega_{rf}C_{gs}, \qquad y_6=j\omega_{rf}C_{gd}, \qquad C\approx 3010^{-12}F, \qquad (8)$$

where C_{gs}, C_{gd} are unipolar transistor parasitic capacitances of gate-source, gate-drain to be found in the reference books, r_{ds} is an equivalent differential output resistance of unipolar transistors [10].

Here we will be looking for the spectral voltage noise density of the amplifier the input of which was connected to the tank circuit, L_TC_T, without the SQUID. In this case $R_i = \omega L_T Q$, where Q is a quality factor of unloading tank circuit. In our calculations we will use t_g=1.3, t_d=1. At first we will calculate the total spectral density of voltage noise $(S_v^{\Sigma})^{1/2}$ on the loading resistor R_1 from all noise sources, and then we will recalculate them to the input of the preamplifier:

$$S_V^{1/2} \simeq (S_V^{\Sigma})^{1/2} / S_1 |Z_{1\sim}|, \qquad (9)$$

where $Z_{1\sim}$ is the complex loading of cascode.

The preliminary calculations have shown that we can ignore the influence of S_{i1}. At any rate the spectral voltage noise density of S_{i1} is not more than 2.5 10^{-10} V/Hz$^{1/2}$. In this case the equivalent scheme becomes simpler, as it is shown in fig. 4. Here

$$Z_{1\sim} \simeq R_1/(1+j\omega_{rf}C_{ds}R_1); \quad Z_1 \simeq 1/[j\omega_{rf}(C+C_{gs}+C_{gd})]; \quad Z_2 \simeq r_{ds}, \qquad (10)$$

where R_1 - the loading resistance of a cascode.

The calculations have shown that the influence of S_i on itself is negligible. However, the influence of S_i is more significant through S_{i4}

$$S_{i4} = [S_2/(1+S_2 r_s)]^2 S_i \, |(Z_2+Z_{1\sim})Z_1/(Z_1+Z_2+Z_{1\sim})|^2, \qquad (11)$$

where $S_i = S_{i2}+S_{i3}+S_{i6}$.

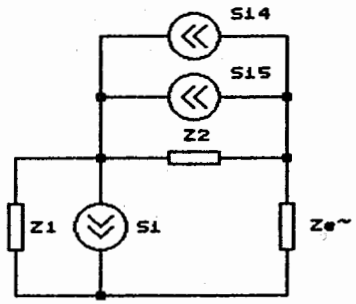

Fig. 4. The transferred equivalent circuit of the cascode input stage.

At $f_{rf}=\omega_{rf}/2\pi$=20 MHz $S_{i4} \simeq 30.6\ 10^{-23} A^2/Hz$.

The total noise on loading resistance

$$S_v^{\Sigma} = (S_{i4}+S_{i5})|Z_2 Z_{1\sim}/(Z_1+Z_2+Z_{1\sim})|^2. \qquad (12)$$

For 20 MHz,

$$S_v^{\Sigma} \simeq (S_{i4}+S_{i5})R_1 \simeq 9.5\ 10^{-16}\ V^2/Hz. \qquad (13)$$

The spectral density of voltage noise recalculated to the input of amplifier is

$$(S_v^p)^{1/2} = (S_v^{\Sigma})^{1/2}/SR_1 \simeq 2\ 10^{-9} V/Hz^{1/2} \qquad (14)$$

The calculations have shown that capacitance of the coaxial line, C ~ 30 pF influences significantly the amplifier gain only at f_{rf} more than 40MHz . And, when f_{rf} is more than 40 MHz it would be better to use another configuration of the first stage, for example, a completely cooled one.

Experiments have shown that at the frequency of 20 MHz our cooled amplifier practically had not decreased total noise of the SQUID system compared with the one operating in the room.

If voltage noise of the the amplifier S_v^p is known, its noise temperature T_p can be found. According to [5],

$$T_p = S_v^p/4k_b\alpha R_T, \qquad (15)$$

where R_T is dynamical resistance of tank circuit coupled with the interferometer.

Owing to the importance of the α parameter for noise calculations in the SQUID system it is necessary to consider the method of its determination in detail.

Slope parameter of "plato" α

The determination of α using the rf-volt-current characteristic has been developed by Jackel and Buhrman [6]. Here it should be noted that this method can be realized with a significant error which does not make it possible to compare correctly experimental results with a theoretical model. This error is caused by the nonlinearities of the amplitude detector D,C,R, and, besides, by the amplitude modulators of rf-generators, particularly, in the region of small values of voltage. Since the main parameter of our SQUIDs usually is low, $\beta \sim 1$, the above mentioned units work just in that region. To escape this error from nonlinearity, one must use some compensation method. The functional scheme illustrating the method used in our experiments is given in fig.5. In fig.5 1 is the superconducting quantum interferometer, 2 is tank circuit inductively coupled to the interferometer, 3 is a rf-bias generator, 4 is a low-noise rf-amplifiers, 5 is an amplitude detector, 6 is the digital-analogue converter giving out linear increasing voltage to the amplitude-modulation

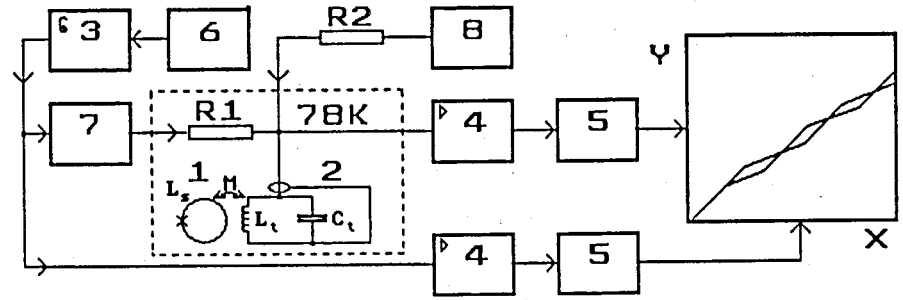

Fig.5. The function scheme to measure slope parameter of the VIC "plato". 1 is a superconducting quantum interferometer, 2 is tank circuit inductively coupled to an interferometer, 3 is the rf-bias generator, 4 is the low-noise rf-amplifiers, 5 is the amplitude detectors, 6 is the digital-analog converter giving out linear increasing voltage to the amplitude-modulation input of the rf-generator, 7 is the rf-attenuator, 8 is the digital-analog converter giving out direct bias current which creates alternate magnetic flux applied to the SQUID: $n\phi_o$, $(n+1/2)\phi_o$, where n is the integer. Digital-analog converters and also reading and representing of information were realized by the IBM-PC/AT.

input of the rf-generator, 7 is the rf-attenuator, 8 is the digital-analogue converter giving out direct bias current which creates alternate magnetic flux applied to the SQUID: $n\phi_o$, $(n+1/2)\phi_o$, where n is the integer. Digital-analogue converters and also the reading and representation of information are realized by the IBM-PC/AT.

Volt-current characteristics measured without and with compensation are shown in fig.6a and fig.6b respectively. The considerable distinctions of these curves are clearly seen.

From fig.6b our SQUIDs with $L_s \sim 10^{-10}$H have α=0.44. According to (15), the noise temperature of the amplifier at 20 MHz is

$$T_p = S_v^p / 4k_b \alpha R_T \simeq 83K.$$

Hence, the equivalent flux noise of rf-preamplifier is $\langle S_\phi^p \rangle \simeq 0.6\ 10^{-4}\ \phi_o/Hz^{1/2}$, and equivalent flux noise created by tank circuit, according to (4), is $\langle S_\phi^{tc} \rangle \simeq 0.6\ 10^{-4} \phi_o/Hz^{1/2}$.

Thus, the major contribution to the total flux noise of the high-T_c SQUID system is made not only by the amplifier as it is typical for the low-T_c one, but also by the tank circuit as well.

Since S_ϕ^{tc} is near to S_ϕ^p the system interferometer-tank circuit is best coupled [5].

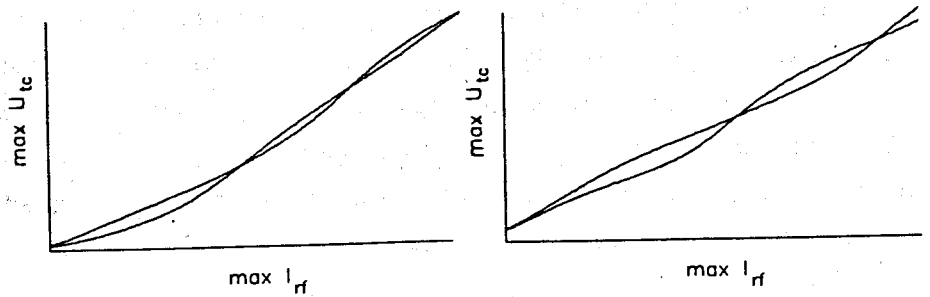

Fig.6. RF-volt-current characteristics of the RF-SQUID: a) is measured without compensation, b) is measured with compensation of nonlinearities.

According to theoretical predictions the noise contributions from all sources can be decreased by ω_{rf} increasing [6]. That have been experimentally confirmed for niobium SQUIDs, e.g., in [11]. We have realized the similar

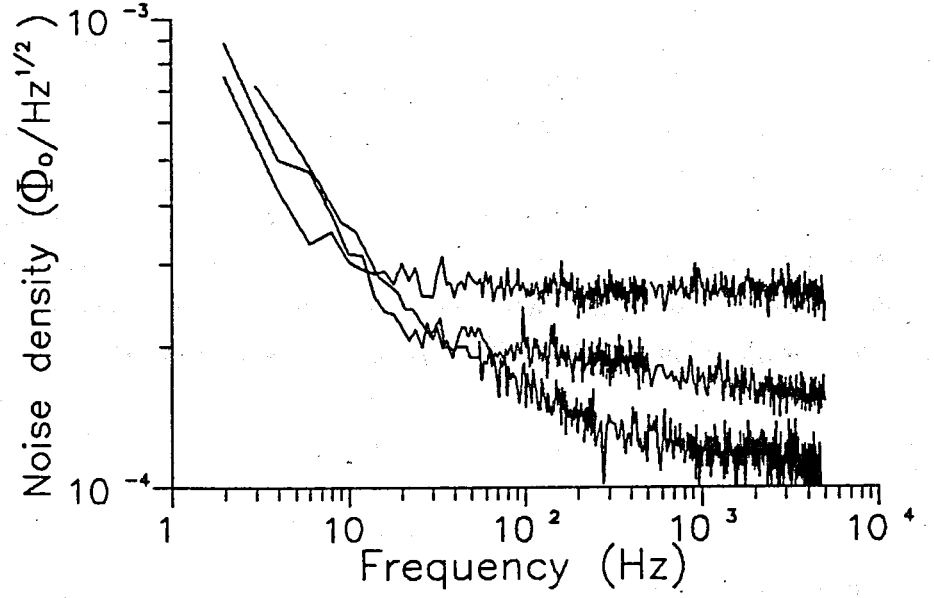

Fig.7. The spectral noise densities of the SQUID system at the different bias frequencies, $\omega_{rf/2\pi}$.

experiment for the high-T_c SQUIDs in frequency bandwidth from 10 to 40 MHz at $k^2Q \sim \pi/2$. The spectral noise density was measured in the output of the SQUID feedback circuit using the standard Fast Furrier Transform procedure. The spectral densities of the magnetic flux measured at 10, 20, 40 MHz respectively are shown in fig.7. Practically a classical result has been received: S_ϕ^Σ is proportional to $1/\omega_{rf}$. That is in good agreement with the Manly-Row expression. This result demonstrates that high-T_c SQUIDs with $L_s \sim L_f$ nevertheless can be classified as parametric elements and, consequently, we can use the estimates, which have already been developed for them.

Conclusion

Naturally, the experimental results mentioned above require the comparison to theoretical models. However, it was

not the purpose of this part of the article. Here we have given only the most important measurement methods and main function units developed for our experiments. Using this information, all scientists will be able to repeat them without difficulties. The essential commentaries will be given in the second part of paper. But it should be noted, that the results described here are sufficient for specialists to perform original analysis and to reach necessary conclusions.

REFERENCES

1. N.V. Zavaritsky et al. Magnetic penetration depth δ_o and critical current density in Y-Ba-Cu-O crystals. Physica C, 1989, v. 162-164, p. 443.

2. O.G. Symko et al. High-T_c superconducting shields. Progress in high temperature Superconductivity, 1989, v. 9, p. 313-314.

3. A.G. Likhachev et al. Magnetocardiometer based on a single-hole high-T_c SQUID. Supercond. Shi. Technol. 1990, v. 3, p. 148-150.

4. V.N. Polushkin. RF-SQUID in the limit of large fluctuations. JINR preprint, 1989, P13-89-201.

5. J. Clarke: Superconducting Quantum Interference Devices for Low Frequency Measurements. Superconducting Applications: SQUID and Machines, Ed. Schwartz. B.B. and Foner. S. (Plenum New York 1977). pp. 67-124.

6. L.D. Jackel, R.A. Buhrman. Noise in the rf-SQUID. J. of Low Temp. Phys., 1975, v. 19, №3/4, p. 201-245.

7. V.N. Polushkin, B.V. Vasiliev. Investigation of rf SQUID behaviour at the liquid nitrogen temperatures. Mod. Phys. Lett. B, 1989, v. 3, №17, p. 1327-1335.

8. B.M. Rogachevski. Superconducting measurement devices. Novosibirsk, 1986, p. 80.

9. N.V. Golyshev et. al. Noise magnetic flux in real rf-SQUIDs. Sov. Priborostroenie, 1987, №5, p. 56-61.

10. Z.N. Musyka. The sensitivity of wireless set devices based on semiconductor elements. Moscow, 1981.

11. J.M. Pierce et al. IEEE Trans. Magn., 1974, MAG-10, p. 599.

Received by Publishing Department
on April 25, 1991.

Полушкин В.Н., Лихачев А.Г. E13-91-193

Тепловые шумы в высокотемпературных радиочастотных сквидах. I. Техника эксперимента

Изложен метод исследования шумовых характеристик сквидовских систем. Приведены функциональные узлы и принципиальные схемы устройств, позволяющие сравнивать экспериментальные результаты с теоретическими моделями. Даны принципиальная схема и расчет собственных шумов охлаждаемого предусилителя для исследования предельного разрешения сквида. Разрешение по энергии при частоте накачки 40 МГц составило $\epsilon \simeq 2{,}3 \cdot 10^{-28}$ Дж/Гц.

Работа выполнена в Лаборатории нейтронной физики ОИЯИ.

Сообщение Объединенного института ядерных исследований. Дубна 1991

Polushkin V.N., Likhachev A.G. E13-91-193

The Thermal Noise in High-T_c RF SQUIDs. I. Experimental Technique

The paper describes the method of investigation of noise characteristics in the SQUID system. The function units and schematics of devices allowing one to compare experimental results to the theoretical model are discussed. The schematic and the noise calculations of the cooled rf-preamplifier which is intended for the investigation of the limit energy resolution are given. The energy resolution of the SQUID system at the bias frequency 40 MHz was $\epsilon \simeq 2.3 \cdot 10^{-28}$ J/Hz.

The investigation has been performed at the Laboratory of Neutron Physics, JINR.

Communication of the Joint Institute for Nuclear Research. Dubna 1991